Interaction of a highly radiative shock with a solid obstacle

M. Koenig, Th. Michel, R. Yurchak, C. Michaut, B. Albertazzi, S. Laffite, E. Falize, L. Van Box Som, Y. Sakawa, T. Sano, Y. Hara, T. Morita, Y. Kuramitsu, P. Barroso, A. Pelka, G. Gregori, R. Kodama, N. Ozaki, D. Lamb, and P. Tzeferacos

Citation: Physics of Plasmas **24**, 082707 (2017); doi: 10.1063/1.4996010

View online: https://doi.org/10.1063/1.4996010

View Table of Contents: http://aip.scitation.org/toc/php/24/8

Published by the American Institute of Physics

Interaction of a highly radiative shock with a solid obstacle

M. Koenig,[1,2] Th. Michel,[1] R. Yurchak,[1] C. Michaut,[3] B. Albertazzi,[1,4] S. Laffite,[5] E. Falize,[5,6] L. Van Box Som,[5,6,7] Y. Sakawa,[8] T. Sano,[8] Y. Hara,[8] T. Morita,[9] Y. Kuramitsu,[10] P. Barroso,[11] A. Pelka,[12] G. Gregori,[13] R. Kodama,[4] N. Ozaki,[4] D. Lamb,[14] and P. Tzeferacos[14]

[1]*LULI - CNRS, Ecole Polytechnique, CEA, Université Paris-Saclay, F-91128 Palaiseau Cedex, France and UPMC Univ. Paris 06, Sorbonne Universités - F-91128 Palaiseau Cedex, France*
[2]*Institute for Academic Initiatives, Osaka University, Suita, Osaka 565-0871, Japan*
[3]*LUTH, Observatoire de Paris, PSL Research University, CNRS, Université Paris Diderot, Sorbonne Paris Cité, 92190 Meudon, France*
[4]*Graduate School of Engineering, Osaka University, Suita, Osaka 565-0871, Japan*
[5]*CEA, DAM, DIF, F-91297 Arpajon, France*
[6]*CEA Saclay, DSM/Irfu/Service d'Astrophysique, F-91191 Gif-sur-Yvette, France*
[7]*LERMA, Observatoire de Paris, PSL Research University, CNRS, Sorbonne Universités, UPMC University Paris 06, F-75005 Paris, France*
[8]*Institute of Laser Engineering, Osaka University, Suita, Osaka 565-0871, Japan*
[9]*Faculty of Engineering Sciences, Kyushu University, 6-1 Kasuga-Koen, Kasuga, Fukuoka 816-8580, Japan*
[10]*Department of Physics, National Central University, Jhongli 320, Taiwan*
[11]*GEPI Observatoire de Paris, PSL Research University, CNRS, Université Paris Diderot, Sorbonne Paris Cité, 75014 Paris, France*
[12]*Helmholtz-Zentrum Dresden - Rossendorf, Bautzner Landstraße 400, 01328 Dresden, Germany*
[13]*Clarendon Laboratory, University of Oxford, Parks Road, Oxford OX1 3PU, United Kingdom*
[14]*Flash Center for Computational Science, University of Chicago, Illinois 60637, USA*

(Received 9 October 2016; accepted 21 June 2017; published online 9 August 2017)

In this paper, we present the recent results obtained regarding highly radiative shocks (RSs) generated in a low-density gas filled cell on the GEKKO XII laser facility. The RS was generated by using an ablator-pusher two-layer target (CH/Sn) and a propagation medium (Xe). High velocity RSs have been generated (100–140 km/s), while limiting as much as possible the preheating produced by the corona emission. Both self-emission and visible probe diagnostics highlighted a strong emission in the shock and an electron density in the downstream gas. The RS characteristics that depend on the initial conditions are described here as well as its precursor interaction with an aluminium foil used as an obstacle. The obtained results are discussed which show a strong extension of the radiative precursor (1 mm) leading to an expansion velocity of the obstacle up to ≈30 km/s compatible to a 20 eV temperature. *Published by AIP Publishing*. [http://dx.doi.org/10.1063/1.4996010]

I. INTRODUCTION

In astrophysics, many phenomena involving strong radiative shocks (RSs) disturb and inject energy into the interstellar medium, affecting the rate of star formation in galaxies. They are referred to as "feedback mechanisms," and studying them is critical to understanding galaxy evolution. Therefore, the interaction of strong radiative shock waves with other structures is a central problem in astrophysics, just as it is in inertial-confinement fusion (ICF) where spherical RSs have been recently observed in cryogenic implosions.[1]

In the interstellar medium, the shock dynamics is closely related to the interaction between radiative structures (radiative shock, Marshak wave) and inhomogeneous/clumpy media. One of the most beautiful examples is the Eagle Nebula in M16, otherwise referred to as the Pillars of Creation. This spectacular phenomenon is commonly seen wherever molecular clouds around massive stars (O and B stars) occur. Such hot stars produce intense UV radiation bathing the surface of nearby molecular clouds, causing ablation or photo-evaporation. The absorbing layers become hot and vaporize, in response to which a strong-shock compression wave is launched into the cloud. Dense evaporating gaseous globules will evolve in stellar nurseries. The proposed formation mechanisms for such pillars usually involve instabilities at the boundary between the cloud and the ionized region, which grow with time.[2–5]

Among the hydrodynamic processes in these structures, strong RSs are a fundamental aspect. The RS corresponds to any shock wave that is fast enough to become radiative.[6] In this case, the structure of the RS depends on the microscopic properties (equation of state and opacity) of the propagation medium. Understanding the physical properties of radiative shock waves is fundamental, since they are the basis for the interpretation of observations of astrophysical phenomena ranging from magneto-spherical accretion in young stellar objects[7] to cataclysmic variables,[8] supernovae, and accreting neutron stars. As a consequence of strong RSs, that is, when a massive flux of photons is produced, the resulting radiative pressure significantly modifies the upstream medium and leads to a totally different hydrodynamic structure. As the shocked structure often becomes optically thick to its own radiation,

Note: Paper submitted as part of the High Energy Density Laboratory Astrophysics (Guest Editor: Siegfried Glenzer). The conference was held at the SLAC National Accelerator Laboratory, Menlo Park, California, 16–20 May 2016.

quantitative data relative to the astrophysical source of these shocks are far and few, and now, it is up to laboratory experiments to help characterize their properties.

Various experiments were conducted in the last decade,[9–13] mainly by the LULI and Michigan groups, and gave valuable highlights on the general structure of highly RSs. The propagation of the shock front compresses and heats the upstream medium so strongly that it leads to the ionization of the gas. By recombination, the ionized gas emits a strong radiation flux that propagates ahead of the shock front and preheats the downstream medium before the compression wave arrives. Depending on the thermodynamical properties of the downstream gas, a specific temperature profile following absorption laws develops ahead of the shock, whereas the density profile stays identical to the classic hydrodynamic case, i.e., a sharp discontinuity.[6] It was first demonstrated that above a threshold shock velocity in xenon gas (as pointed out by Bouquet *et al.*[14]), a radiative precursor develops, and its spatial extension and electron density were measured.[9] Then, more studies were performed on the LULI2000 facility,[10,11] where the fundamental parameters of RSs (temperature, radial expansion, electron density, shock, and precursor velocities) were measured simultaneously. This allowed showing the importance of 2D radiative losses that significantly reduce the shock temperature. In parallel, the Michigan group performed several RS experiments on the OMEGA laser showing the radiative collapse of the shock front,[12] and the strong interaction with walls when the propagation container (tube) has a small radial dimension compared with the shock itself.[13] Astronomical observations can be usually considered as snapshots due to the large time scales involved. So, experiments are the only opportunity to follow the time evolution of a radiative shock and validate radiation hydrodynamic astrophysical simulations.

Recent theoretical studies[15,16] proposed a classification of the radiative regimes based on 4 dimensionless parameters: the optical depth τ, the cooling parameter χ (ratio of the cooling time t_{cool} over the hydrodynamic time t_{hydro}), the Boltzmann number Bo (ratio of the enthalpy flux F_{enth} over the radiative flux F_{rad}) and what we will call the Mihalas number R (ratio of the internal energy density E_{int} over the radiative energy density E_{rad}). The shock is considered as radiatively dominated when Bo is much lower than 1 and R is close to 1. In this context, astrophysicists need radiative experiments to be performed in order to validate modeling the various objects where this radiation physics occurs. Up to now, most analytical works rely on a steady-state hypothesis,[14] and radiation transport is often simplified in order to speed up calculations. Laboratory astrophysics experiments are therefore extremely valuable to benchmark codes and models therein. In particular, the usual way to treat radiation in simulation codes (diffusion approximation) was adequate up to now to reproduce the experimental results as all were performed within the optically thick regime. This is not always the case in astrophysical situations, and a more accurate comparison between simulation codes and experimental data in the optically thin regime remains fundamental and is not yet been studied in detail.

To this end, in this paper, we aimed to look in more detail on the RS structure and the strength of the associated radiative precursor. Herein, we report on new experimental results where a dedicated solid target was designed to enhance the shock velocity in xenon gas, increasing the radiation effects. For this new type of RS experiment, we also aimed to infer the processes involved in the interaction between radiation coming from the RS and a spherical obstacle as a mock-up of the ablation processes in molecular clouds or similar objects. To achieve this, we have generated on the GEKKO XII facility, a strong radiative shock in a dedicated gas-cell setting the shock in a flux-dominated regime, i.e., where $Bo < 1$ and $R > 1$. These RSs exhibit a well-known radiative precursor in the upstream medium. We used a long generated precursor to observe its interaction with a solid foil. Optical diagnostics were carefully set up in order to measure all possible parameters related to strong RSs. We clearly observed a set in motion of this foil due to absorption of the radiation emitted by the strong RSs. From the measured expansion velocity, we inferred the associated temperature to be $\approx$20 eV.

II. EXPERIMENTAL SETUP

This experiment was performed on the GEKKO XII laser facility (Institute of Laser Engineering, Osaka University, Japan) that allowed using up to 1 kJ at 3ω of laser energy. The high number of laser beams available permitted having a wide range of energy deposited on the target. Three to six beams were used to irradiate the target, delivering 400 J to 1200 J of laser light in a 500 ps Gaussian pulse at a wavelength of 351 nm. The focal spot size was around 350–400 μm leading to laser intensities ranging from 4.0×10^{14} W/cm2 to 1.5×10^{15} W/cm^2.

We have used a well-known target design previously described[10,17] that was adapted to our specific needs. Here, we could insert, on the back of the cell, an aluminum foil to infer its ablation by the strong and long radiative precursor generated by the main solid target in the xenon gas. The pusher launching the strong shock was composed of 25 μm CH, as an ablation layer, and 4 μm Sn, as an X-ray shield against radiation produced in the hot corona. As soon as the shock breaks out on the rear side of the titanium layer, it propagates in the low-density gas confined in the cell having transverse windows transparent to visible light. The gas material and its density (xenon at P = 50 mbar) were chosen such that to maximize the radiation effects according to common dimensionless numbers.[16] In this new experiment, we wanted to study the interaction of a RS (radiative precursor) with a solid obstacle in order to measure the influence of the radiative precursor, its strength and its spread. To this end, a 20 μm thick aluminum foil was placed at 2 mm from the ablator-pusher layer (Fig. 1).

On the Gekko XII laser facility, we were able to use the large array of visible diagnostics implemented as presented in Fig. 2. First, optical pyrometry diagnostics recorded (either streaked or gated with GOI) the shock or precursor self-emission. Having a short bandwidth blue interferential filter, the brightness temperature can be deduced after careful calibration. Besides the driving beams, a few mJ, 527 nm, 10 ns laser probed the gas cell in the direction perpendicular to the shock propagation. Two sets of diagnostics were set-up here: a modified Nomarski interferometer coupled to another GOI or ISTAR to infer the change in the electron

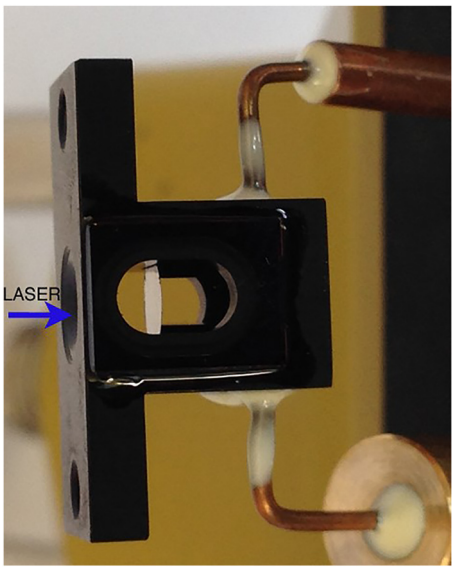

FIG. 1. The RS target with the 20 μm aluminum foil placed at 2 mm from the Sn pusher positioned at the edge of the window on the laser side.

density due to the ionisation of the xenon gas in front of the RS. A simple shadowgraph coupled to a streak camera allowed following in time the probe laser absorbing density ($ne \leq 10^{19}\,cm^{-3}$) position in front of the aluminium foil.

The streaked visible diagnostics implemented (self-emission or shadowgraphy) allowed measuring, on each shot, the shock or precursor velocities (up to 140 km/s) in the 50 mbar xenon gas filled cell. The two streaked visible diagnostics are fundamental to constraining the shock conditions in the gas to be reproduced by simulations. The velocities, associated to the range of intensities used in this experiment, measured by SOP and streaked shadowgraphy, varied between 80 and 140 km/s. In Fig. 3, we plotted the simulated values obtained with the 1D radiative hydrodynamic code MULTI (red squares) and the 2D code FLASH (green filled rhombus).

We observed good agreement between our experimental results and 2D simulations that made us confident to use this code to infer other parameters, such as temperature, in the shock front that are necessary to determine the dimensionless numbers. We also observe that at high intensities (above 5×10^{14} w/cm^2), the velocities given by MULTI are overestimated. This is due to both the 2D Gaussian shape of the

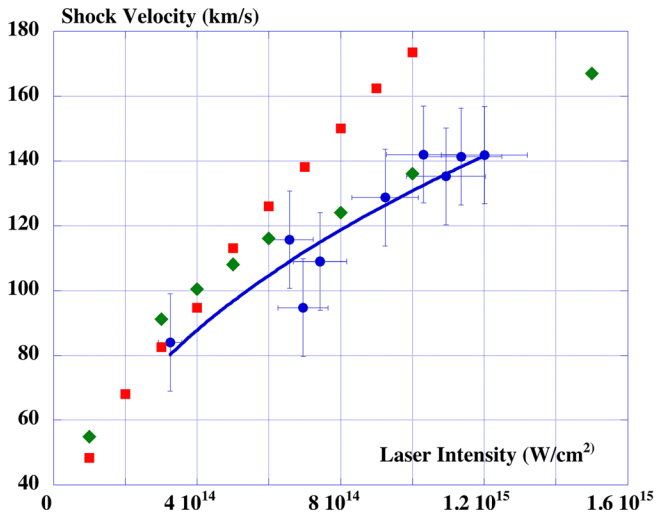

FIG. 3. Comparison of measured velocities (blue filled circle) and 1D (red squares) and 2D simulations (green filled rhombus).

focal spot and 2D radiation losses that are not taken into account as already pointed out in a previous paper.[10]

This good agreement gave us confidence in our simulation capabilities on the hydrodynamics, therefore leading to accurate determination of the two dimensionless numbers *Bo* and R versus the measured shock velocity for the Gekko shots (Fig. 4) according to recent work.[16] As compared to a previous work,[10] we approached in the Gekko experiment a regime where R was about 20–50, *Bo* being the order of several 10^{-2}. Indeed, the Boltzmann number *Bo* is much lower than 1, meaning that the radiative flux is higher than the thermal one. However, we begin to be close to the case where the radiative energy might influence the shock and the precursor behavior.

Having good constraint on the RS strength through the velocity measurements and confidence in our simulation capabilities on the hydrodynamics, we placed an aluminum foil at a distance of 2 mm from the ablator-pusher bilayer target (Fig. 1). Then, we studied in detail on the interaction of the intense x-ray flux coming from the RS front with the aluminum foil and examined all possible processes involved in its ablation. Two main diagnostics are relevant here: the interferometry (Fig. 5) coupled to a GOI that provides the electron density in the precursor along the shock propagation and the streaked

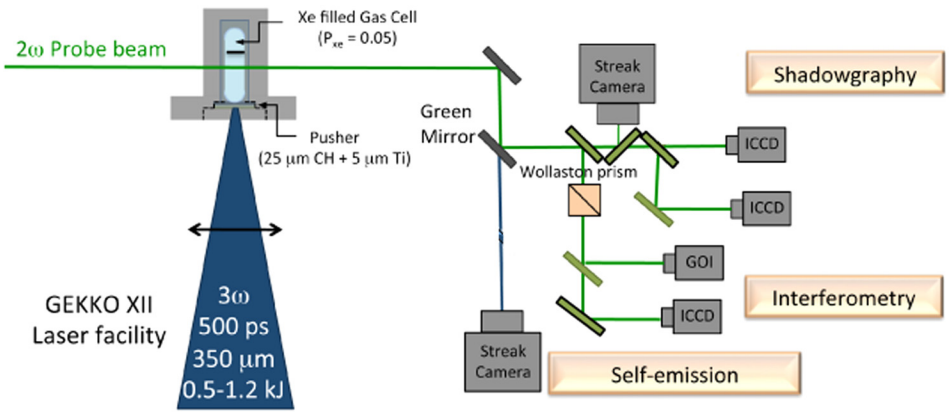

FIG. 2. General setup of the experiment including target and visible diagnostics.

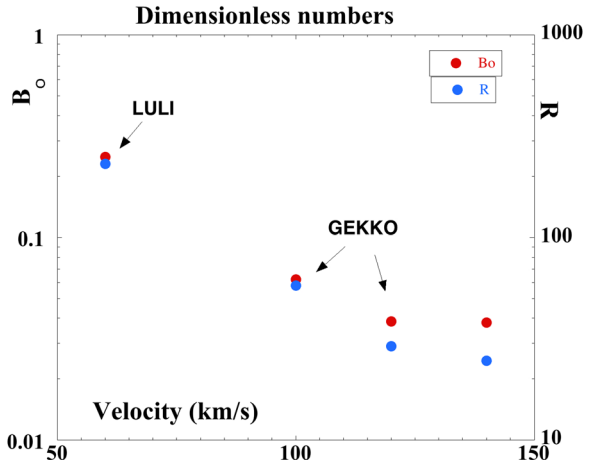

FIG. 4. Boltzmann (*Bo*—blue filled circle) and Mihalas (R—red filled circle) numbers in RS experiments at LULI[10] and in the new experiment versus the measured shock velocity.

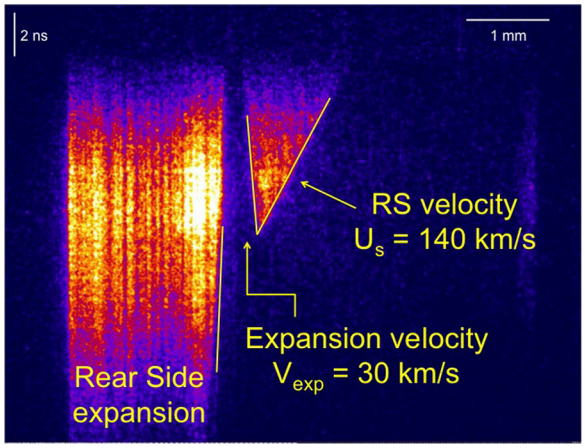

FIG. 6. Streaked transverse shadowgraphy of the RS and the aluminum foil.

shadowgraphy that allows infering the aluminum surface expansion versus time (Fig. 7). In Fig. 5, we show a synthetic reconstruction of the experimental 2D interferometer obtained using neutrino software (http://web.luli.polytechnique.fr/Neutrino) developed in the LULI laboratory. We can observe the position of the RS front that is opaque to the 2ω probe beam. We also see the strong perturbation of the fringes ahead of the shock front due to the radiative precursor that ionizes the xenon gas. The foil, positioned 2 mm from the initial solid target, also presents some deformation. While the interfringe used here was a little bit too large to obtain a detailed expansion of the aluminum foil, deformations near its position can still be observed. Following an Abel inversion, assuming a cylindrical symmetry, we deduced the electron density along the shock propagation (Fig. 5). Here, the precursor extends up to 1 mm after the shock front, typical of optically thin medium to radiation coming from the shock. We also observe a clear increase of the electronic density near the aluminum foil, indicating its expansion toward the incoming RS. For this particular shot, the shock velocity was $\approx$100 km/s, as we used only 3 beams of the Gekko laser and its temperature is $\approx$20 eV. Following the electron density profile [Fig. 5(b)] and the initial ion density (50 mbar of xenon), we can deduce the ionization stage in the radiative precursor that goes from 5 to 3 depending on the position in the cell. According to the SESAME tables,[18] this corresponds to the precursor temperature ranging from 10 to 5 eV.

In order to determine the expansion velocity, we used the streaked shadowgraphy diagnostic as described previously. The time window is limited to 20 ns as the 2ω probe beam has a FWHM pulse duration of less than 20 ns. The shadowgraphy diagnostic provides us the RS velocity, following the position of the RS and its precursor propagating in the xenon gas. The RS is the frontier between the completely opaque and the low light level of the probe beam (from right to left) as actually the precursor density is low enough, so that the laser light can go through (slightly absorbed) as the RS completely absorbs the probe laser beam. Following this frontier until the RS reaches the expanding aluminum foil (Fig. 6) we determine a velocity of 140 km/s. By carefully looking at the obstacle foil expansion (a clear border between completely opaque and bright light along the foil), we deduced its maximum velocity in this particular case to be $\approx$30 km/s. For this shot, the laser intensity was 10^{15} W/cm^2, slightly higher than expected, showing a large influence of the radiation escaping from the shock front.

Indeed, we clearly observe in Fig. 6 that, a few nanoseconds after the main drive beams, the aluminum foil already expands toward the RS. However, due to the large intensity, some preheating due to hard x-rays coming from the hot corona also heats up the aluminum foil before the main precursor reaches it. We pay particular attention to this problem

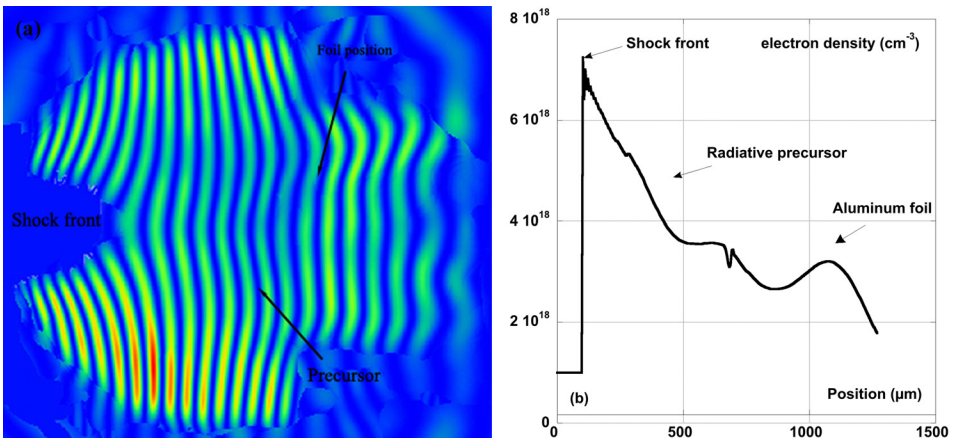

FIG. 5. 2D synthetic reconstructed interferogram of the radiative shock at t = 8 ns (a) and the associated electron density along the shock propagation in the Xe gas (b).

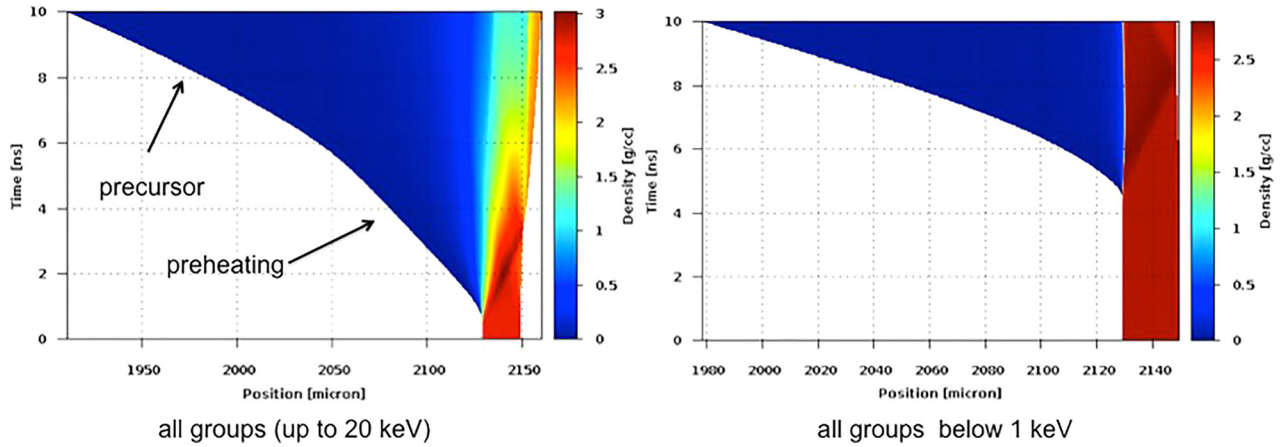

FIG. 7. Simulations of the aluminum obstacle situated at 2 mm from the main target. On the left, all groups up to 20 keV are included in the radiation transport. On the right, a cutoff at 1 keV has been made to reduce preheating.

by performing dedicated 1D simulations by artificially cutting the groups that are responsible for foil preheating (E> 1 keV). The results are presented in Fig. 7, where we can observe, for a numerical laser intensity of 7×10^{14} W/cm^2, an initial expansion of the aluminum foil (when all radiation is on) at a velocity of about 5–10 km/s, corresponding to a 1–2 eV initial temperature according to a simple unloading model. However, the maximum expansion velocity in both cases (with and without groups over 1 keV) is similar, and ≈30 km/s in this particular case, and it is mainly due to the interaction of the RS precursor with the obstacle.

By varying the laser intensity on several shots, we could determine the expansion velocity as reported in Fig. 8. This value increases with laser intensity as expected and can be compared to 1D and 2D simulations. Here, we observe a clear discrepancy between experimental data and the 1D simulations that obviously overestimate the expansion velocity due to no lateral radiation losses as mentioned before. However, the present 2D FLASH simulations seem to underestimate this velocity probably partly due to an inaccurate treatment of initial preheating or other phenomena. When looking at the trajectory of the aluminum foil expansion (Fig. 9), we can observe that the trend is very similar for both electron densities ne = 10^{19} and 10^{20} cm^{-3} that are relevant to the probe beam to be absorbed by the aluminum plasma. But the velocities are still too low even if it increases when the density limit decreases as expected. After 10 ns, the aluminum foil reaches a velocity of about 30 km/s. By assuming that the foil expansion is adiabatic, the measured velocity (sound velocity) corresponds to a temperature of about 20–30 eV. A simple estimation can be made to infer the radiative flux emitted by the shock in the xenon gas. Let us consider that it emits like a black body (σT^4); after considering the geometric dilution and the propagation of radiation through the gas, we can quantify the incident power on the obstacle. For a 1 mm distance between the shock front (having 30 eV temperature) and the aluminum foil, the incident power on the obstacle is a few 10^{10} W/cm^2. Taking into account the absorption of this radiative flux by the aluminum surface with time, one obtains an expansion very similar to the measured one (30 km/s) when the shock almost impacts the foil.

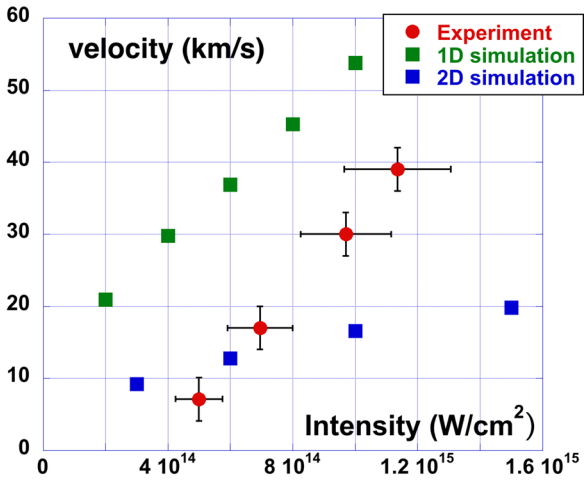

FIG. 8. Foil expansion given by 1D (green filled square) and 2D (blue filled square) simulations compared to experimental results (red filled circle).

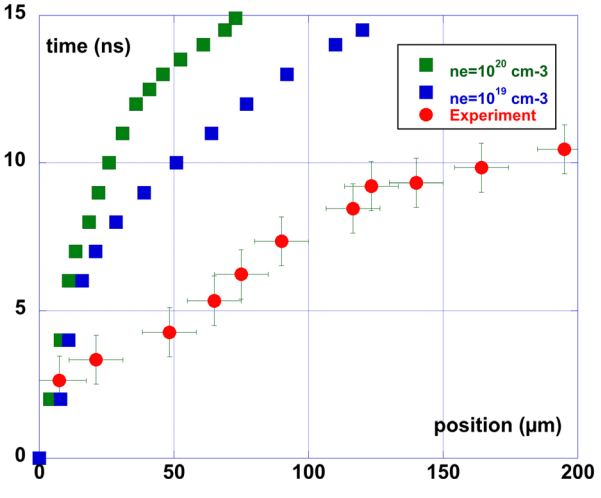

FIG. 9. Foil expansion versus time in 2D simulations for the electron density of $n_e = 10^{20}$ cm^{-3} (green filled square) and 10^{19} cm^{-3} (blue filled square) compared to experimental results (red filled circle).

III. CONCLUSIONS

In this paper, we report for the first time, a clear observation of the interaction of the radiative flux with a solid obstacle. The radiative shock is generated in xenon gas after the breaking of a strong shock produced in a two-layer solid foil by laser beams having intensities ranging from 4×10^{14} W/cm^2 to 1.2×10^{15} W/cm^2. The obstacle is a 20 μm aluminium foil, set in 50 mbar xenon gas and situated 2 mm from the solid ablator-pusher. We accurately measured the RS velocities under different conditions up to 140 km/s allowing determining the Boltzmann and Mihalas dimensionless numbers. In this experiment, we achieved the intermediate regime as previously described:[10] the radiative flux is much higher than the thermal one, with the radiative energy being not high enough to be in a fully radiative regime. However, for the highest velocity (140 km/s), the Mihalas number $R = 25$, meaning that we will potentially reach in the future the case where the radiative energy can slightly modify the shock structure ($R < 10$). Moreover, we tried to determine the strength of the radiation flux by positioning the aluminium foil at 2 mm from the main solid pusher target. A clear expansion of the surface toward the shock propagation in xenon is observed with a maximum velocity of 30 km/s and a temperature of 20–30 eV. Further experiments will be performed, especially on a higher energy laser (LMJ) in 2018 that will provide higher velocities (typically 200 km/s), giving lower Boltzmann and Mihalas numbers, thereby enhancing the radiation flux and energy.

ACKNOWLEDGMENTS

Part of this work was supported by the "Programme National de Physique Stellaire" (PNPS) of CNRS/INSU, France and the Scientific Council of the Observatoire de Paris. This work was also strongly supported by the COST action MP1208. We also acknowledge ILE (Institute of Laser Engineering, Osaka University, Japan) for a multi-year collaborative research program.

[1]A. Pak, L. Divol, G. Gregori, S. Weber, J. Atherton, R. Bennedetti, D. K. Bradley, D. Callahan, D. T. Casey, E. Dewald, T. Doppner, M. J. Edwards, J. A. Frenje, S. Glenn, G. P. Grim, D. Hicks, W. W. Hsing, N. Izumi, O. S. Jones, M. G. Johnson, S. F. Khan, J. D. Kilkenny, J. L. Kline, G. A. Kyrala, J. Lindl, O. L. Landen, S. Le Pape, T. Ma, A. MacPhee, B. J. MacGowan, A. J. MacKinnon, L. Masse, N. B. Meezan, J. D. Moody, R. E. Olson, J. E. Ralph, H. F. Robey, H. S. Park, B. A. Remington, J. S. Ross, R. Tommasini, R. P. J. Town, V. Smalyuk, S. H. Glenzer, and E. I. Moses, Phys. Plasmas **20**(5), 056315 (2013).
[2]L. Spitzer, Astrophys. J. **120**(1), 1 (1954).
[3]E. A. Frieman, Astrophys. J. **120**(1), 18–21 (1954).
[4]R. J. R. Williams, D. Ward-Thompson, and A. P. Whitworth, Mon. Not. R. Astron. Soc. **327**(3), 788–798 (2001).
[5]A. Mizuta, J. O. Kane, M. W. Pound, B. A. Remington, D. D. Ryutov, and H. Takabe, Astrophys. J. **621**(2), 803–807 (2005).
[6]Y. B. Zeldovich and Y. P. Raizer, *Physics of Shock Waves and High Temperature Hydrodynamic Phenomena* (Academic Press, New York, 1967).
[7]S. Orlando, R. Bonito, C. Argiroffi, F. Reale, G. Peres, M. Miceli, T. Matsakos, C. Stehle, L. Ibgui, L. de Sa, J. P. Chieze, and T. Lanz, Astron. Astrophys. **559**, A127 (2013).
[8]C. Busschaert, E. Falize, C. Michaut, J. M. Bonnet-Bidaud, and M. Mouchet, Astron. Astrophys. **579**, A25 (2015).
[9]S. Bouquet, C. Stéhlé, M. Koenig, J.-P. Chièze, A. Benuzzi-Mounaix, D. Batani, S. Leygnac, X. Fleury, H. Merdji, C. Michaut, F. Thais, N. Grandjouan, T. Hall, E. Henry, V. Malka, and J.-P. J. Lafon, Phys. Rev. Lett. **92**(22), 225001 (2004).
[10]M. Koenig, T. Vinci, A. Benuzzi-Mounaix, N. Ozaki, A. Ravasio, M. R. le Glohaec, L. Boireau, C. Michaut, S. Bouquet, S. Atzeni, A. Schiavi, O. Peyrusse, and D. Batani, Phys. Plasmas **13**(5), 056504 (2006).
[11]T. Vinci, M. Koenig, A. Benuzzi-Mounaix, C. Michaut, L. Boireau, S. Leygnac, S. Bouquet, O. Peyrusse, and D. Batani, Phys. Plasmas **13**(7), 010702 (2006).
[12]A. B. Reighard, R. P. Drake, D. K. K, D. J. Kremer, M. Grosskopf, E. C. Harding, D. R. Leibrandt, S. G. Glendinning, T. S. Perry, B. A. Remington, J. Greenough, J. Knauer, T. Boehly, S. Bouquet, L. Boireau, M. Koenig, and T. Vinci, Phys. Plasmas **13**(8), 082901 (2006).
[13]F. W. Doss, H. F. Robey, R. P. Drake, and C. C. Kuranz, Phys. Plasmas **16**(11), 112705 (2009).
[14]S. Bouquet, R. Teyssier, and J. P. Chièze, Astrophys. J. Supp. **127**(2), 245 (2000).
[15]R. P. Drake, Astrophys. Space Sci. **298**, 49–59 (2005).
[16]C. Michaut, E. Falize, C. Cavet, S. Bouquet, M. Koenig, T. Vinci, A. Reighard, and R. P. Drake, Astrophys. Space Sci. **322**(1-4), 77–84 (2009).
[17]A. B. Reighard, R. P. Drake, K. K. Dannenberg, D. R. Leibrandt, D. Kremer, S. G. Glendinning, T. S. Perry, H. F. Robey, B. A. Remington, R. J. Wallace, D. D. Ryutov, J. Greenough, J. Knauer, S. Bouquet, L. Boireau, A. Calder, R. Rosner, B. Fryxell, D. Arnett, M. Koenig, and J. Stone, in *4th IFSA Conference* (Biarritz, France, 2005).
[18]SESAME: The LANL Equation of State database, Report No. LA-UR-92-3407, 1992.